Transient Responses of Northern Hemisphere Wintertime Circulation to Stratospheric Soot Injection

Simchan Yook[1]*, Kane Stone[1], Joonsuk M. Kang[2], and Jaeyoung Hwang[3]

Affiliations:

[1] Department of Earth, Atmospheric and Planetary Sciences, Massachusetts Institute of Technology, Cambridge, MA, USA

[2] Columbia University, New York, NY, USA

[3] Georgia Institute of Technology, Atlanta, GA, USA

* Corresponding author. Email: syook@mit.edu

Abstract:

Stratospheric aerosol injections are known to strengthen the wintertime polar vortex, with earlier studies linking this response to enhanced equator-to-pole temperature gradients from aerosol heating and the associated thermal-wind balance. However, the mechanisms governing the short-term circulation response remain poorly understood. Here, we use a chemistry-climate model to simulate regional nuclear war scenarios and examine the heat and momentum budgets to quantify the transient thermal and dynamical responses to the tropical soot injection. The results reveal that the enhanced temperature gradients in the mid-to-high latitudes arise not from direct radiative forcing but from dynamical heat redistribution. Together, these findings provide a new perspective — a direct dynamical mechanism — showing that the circulation responses to stratospheric aerosol perturbations, through the redistribution of heat and momentum to remote regions, can play a key role in strengthening the winter polar jet,

Key Points:

- Aerosol perturbations drive tropical temperatures via radiation and extratropical changes via atmospheric dynamics.
- Enhanced meridional temperature gradients in mid-to-high latitudes explain polar vortex intensification via thermal wind balance.
- Dynamical processes play a key role in these enhanced meridional temperature gradients in mid-to-high latitudes.

Plain Language Summary:

Simulations of large-scale nuclear conflicts indicate that substantial injections of aerosols into the stratosphere can strengthen the wintertime polar vortex. Previous studies attributed this strengthening to enhanced equator-to-pole temperature differences caused by aerosol heating, but the detailed dynamical processes remained unclear. Using the Whole Atmosphere Community Climate Model (WACCM) to simulate regional nuclear war scenarios, we show that aerosols influence stratospheric temperatures both directly, through tropical heating, and indirectly, via changes in atmospheric circulation. These dynamical adjustments redistribute heat toward higher latitudes, enhancing meridional temperature gradients and strengthening the polar vortex. The results provide new insight into how aerosol radiative effects in one region can remotely influence stratospheric circulation, highlighting the critical role of atmospheric dynamics in the atmospheric response to large-scale aerosol perturbations.

Main Text:

1. Introduction

The Northern Hemisphere (NH) atmospheric circulation response to stratospheric aerosol injections (SAI) has been extensively examined across a wide range of numerical modeling studies. Simulations of explosive volcanic eruptions (Graf et al., 1991; Bittner et al., 2016; Dalla Santa et al., 2019) and geoengineering scenarios (Banerjee et al., 2021; Jones et al., 2020) typically implement massive injections of sulfur dioxide into the stratosphere. Nuclear war scenarios consider large injections of black carbon (BC) from urban fires (Coupe and Robock, 2021). Results from these studies consistently indicate a broadly similar outcome: aerosol-induced heating of the tropical stratosphere followed by a strengthening of the stratospheric polar vortex (SPV).

A variety of radiative and dynamical mechanisms have been proposed to explain the linkage between tropical aerosol perturbations and the strength of the SPV.

(1) **Direct radiative mechanism:** The first mechanism involves warming of the tropical stratosphere due to aerosol-induced heating, which enhance the meridional temperature gradient and thereby strengthen the stratospheric jet through thermal wind balance (Graf et al., 1993; Kodera, 1994; Robock and Mao, 1995; Coupe and Robock, 2021).

(2) **Indirect dynamical mechanism:** However, some studies suggest that the changes in the stratospheric temperature gradient from the direct radiative effects of aerosol forcing are largely confined to the subtropics. Thus, the acceleration of the jet required to maintain thermal wind balance occurs mainly in the subtropical jet rather than the polar jet. The second mechanism has been proposed to explain the strengthening of the SPV through an indirect dynamical process, the acceleration of the subtropical jet deflects planetary wave

propagation equatorward (i.e., limits poleward wave fluxes), thereby indirectly intensifying the SPV (Toohey et al., 2014; Bittner et al., 2016; Dalla Santa et al., 2019).

(3) **Indirect radiative mechanism:** The third mechanism includes an indirect tropospheric pathway. Aerosol scattering of shortwave radiation cools the surface, weakens the tropospheric meridional temperature gradient and baroclinicity, which in turn, reduces upward wave flux and contributes to the polar jet acceleration (Graf et al., 1992; Stenchikov et al., 2002; Dalla Santa et al., 2019).

Together, these mechanisms highlight how coupled radiative and dynamical adjustments can strengthen the wintertime SPV following tropical aerosol injections. However, most previous work has focused on seasonal or longer-term adjustments. The transient evolution during the weeks immediately following injection - the period when the atmosphere adjusts most rapidly - remains comparatively unexplored.

Here, we use a chemistry-climate model to examine how radiative and dynamical processes contribute to the short-term, stratospheric response to soot injection in regional nuclear-war scenarios. We quantify the evolution of the heat and momentum budgets to assess the processes that link the initial aerosol perturbation to the early-stage circulation response.

2. Data and Methods

2.1. Model and Scenarios

We assess the Whole Atmosphere Community Climate Model version 4 (WACCM4; Marsh et al., 2013) simulations, previously run by Yook et al. (2025) to assess the climate response to a regional nuclear conflict. The simulations are run with fully interactive chemistry and coupled ocean, land, and sea-ice components, with a horizontal resolution of 1.9° × 2.5°, 66 vertical levels, and a model top near 140 km. The model incorporates the Model for Ozone and Related Chemical Tracers (Kinnison et al., 2007) and computes photolysis rates using the Tropospheric Ultraviolet and Visible (TUV) radiation scheme (Madronich & Flocke, 1997), allowing for the effects of aerosol scattering and absorption on actinic fluxes.

Two sets of simulations are analyzed: 1) a control (**CTRL**) case with present-day background conditions and 2) an India-Pakistan (**IP**) case representing a regional nuclear conflict scenario following Yook et al. (2025). In the **IP** experiment, a total of ~6.7 Tg of smoke is injected into the upper troposphere (150-300 hPa) over the India and Pakistan regions during 12-15 January of the first simulation year, consistent with emission estimates from Toon et al. (2007, 2019). The injected smoke consists of 70 % black carbon (BC) and 30 % organic carbon (OC) and is simulated with the Community Aerosol and Radiation Model for Atmospheres (CARMA; Bardeen et al., 2008), which explicitly represents coagulation, wet and dry deposition, and gravitational settling. Details of the model configuration and experimental design are described in Bardeen et al. (2021) and Yook et al. (2025).

Each set of experiments includes 20 ensemble members, initialized from different initial conditions on 1 January to isolate circulation responses to stratospheric aerosol forcing from internal climate variability. All ensemble members were integrated for four months, and the results presented here are based on the ensemble mean of each field.

2.2. The Zonal Mean Heat Budget

To assess the thermal and dynamical responses of the circulation, we quantify the temporal and spatial evolution of the stratospheric heat budget as a function of latitude and pressure (e.g., Holton, 2004; Lachmy & Kaspi, 2020; White et al., 2024). The prognostic equation for zonal mean temperature can be written as:

$$\frac{\partial \bar{T}}{\partial t} = \bar{Q} - \bar{\omega}\left(\frac{\partial \bar{T}}{\partial p} - \kappa\frac{\partial \bar{T}}{p}\right) - \frac{1}{a\cos\phi}\frac{\partial\left(\cos\phi\left(\overline{v'T'}\right)\right)}{\partial\phi} - \left\{\left(\frac{\partial\left(\overline{\omega'T'}\right)}{\partial p} - \kappa\frac{\left(\overline{\omega'T'}\right)}{p}\right) - \bar{v}\frac{\partial\bar{T}}{a\partial\phi} + \overline{Q_{GW}}\right\} \dots (1)$$

TEND RAD ADIA EHFC RES

Here, T is temperature, v is meridional wind, ω is vertical velocity in pressure coordinates, Q is the diabatic heating tendency, and Q_{GW} represents the heating rate due to gravity-wave drag. p is pressure, ϕ is latitude, $a$is Earth's radius, and $\kappa = R_d/c_p$. The overbar denotes the zonal mean, and the prime denotes deviations from the zonal mean.

The term on the left-hand side of the above equation represents the net temperature tendency (TEND). The first term on the right-hand side represents the diabatic heating from the sum of longwave and shortwave heating rates (i.e., radiative processes; RAD). The second term represents the adiabatic process by vertical motion (hereafter ADIA), and the third term corresponds to the meridional eddy heat flux convergence (EHFC). The remaining terms (fourth through sixth) represent heating due to vertical eddy heat flux convergence, temperature advection by the zonal mean meridional wind, and heating from gravity wave drag, respectively, comprising the residual terms (RES). To distinguish heating from dynamical processes from that due to radiative processes, we define the dynamical temperature tendency (DYN) as the sum of the ADIA, EHFC, and RES terms.

3. Results

3.1. Stratospheric Temperature and Circulation Responses

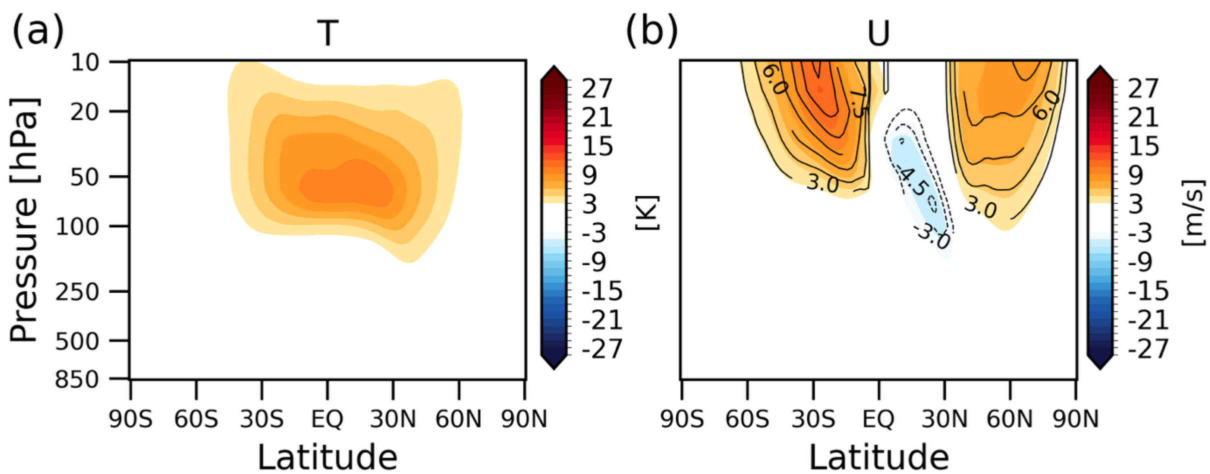

Figure 1. Changes in zonal-mean (a) temperature and (b) zonal wind between **IP** and **CTRL** simulations (color shading). In panel (b), line contours indicate zonal-wind changes estimated from the thermal wind relationship using the temperature anomalies shown in panel (a). All fields are averaged over the 30-day period from 11 January to 9 February.

Figure 1 shows the stratospheric climate responses to the aerosol emission from the IP conflict, including changes in (a) temperature and (b) zonal wind.

The stratosphere warms rapidly after the injection, with temperature anomalies exceeding 10 K in the tropical lower stratosphere during the first month (Fig. 1a). This tropical warming arises primarily from shortwave absorption by black-carbon aerosols, consistent with earlier studies of nuclear-conflict scenarios (Robock et al., 2007; Mills et al., 2008, 2014; Bardeen et al., 2021; Yook et al., 2025).

The circulation responses are marked by strengthening of the wintertime polar vortex. Zonal-wind anomalies show robust westerly accelerations across the NH mid-to-high latitudes as well as over the SH subtropics (Fig. 1b). The thermal-wind response derived from the temperature anomalies (line contours) closely matches the simulated wind response (shading), indicating that the circulation anomalies are largely in thermal-wind balance with the temperature anomalies.

A notable distinction from earlier stratospheric aerosol-injection studies (Bittner et al., 2016a; Toohey et al., 2014) is that our results only show strengthening of the polar jet, with no corresponding strengthening of the subtropical jet. Thus, the second mechanism proposed in earlier works - where an enhanced subtropical jet deflects planetary-wave propagation equatorward, thereby strengthening the SPV- is not applicable here.

The close consistency between the simulated zonal wind response and the thermal wind balance suggests that the primary mechanism in our case may be consistent with the first mechanism: direct thermal perturbations in the stratosphere that intensify the polar night jet through thermal wind balance. We further examine this by quantifying the associated heat-budget in the next section to identify the processes contributing to the polar-jet intensification.

3.2. Stratospheric Heat Budget Analyses

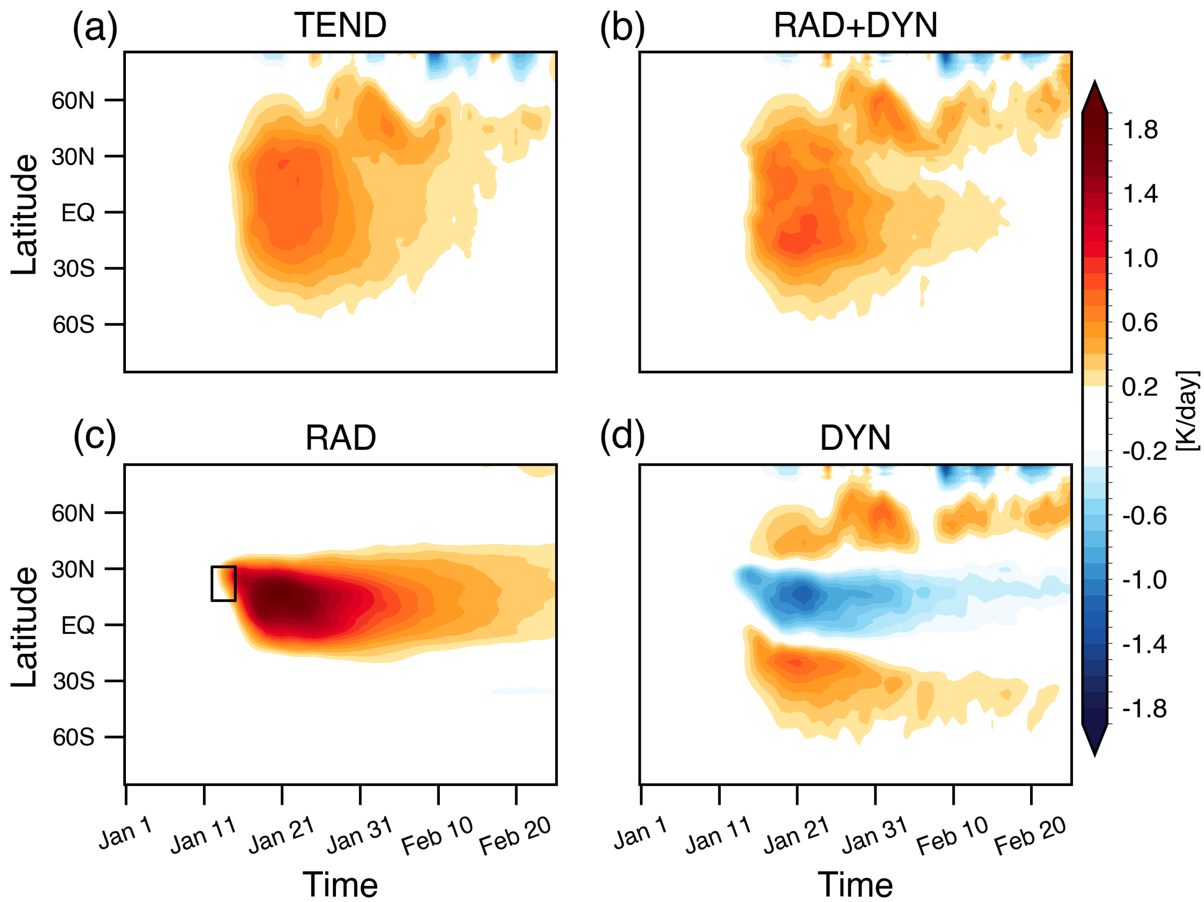

Figure 2. Time series of changes in temperature tendency (K day^{-1}). Each panel shows (a) total temperature tendency (TEND; LHS of Eq. 1), (b) sum of all diagnosed thermodynamic tendency terms (RAD+DYN; RHS of Eq. 1). (c) radiative heating term (RAD), and (d) dynamical contribution (DYN). All results in Figs. 2-4 are shown as differences between the **IP** and **CTRL** simulations. The black box in panel (c) marks the aerosol injection time and location for the IP conflict scenario.

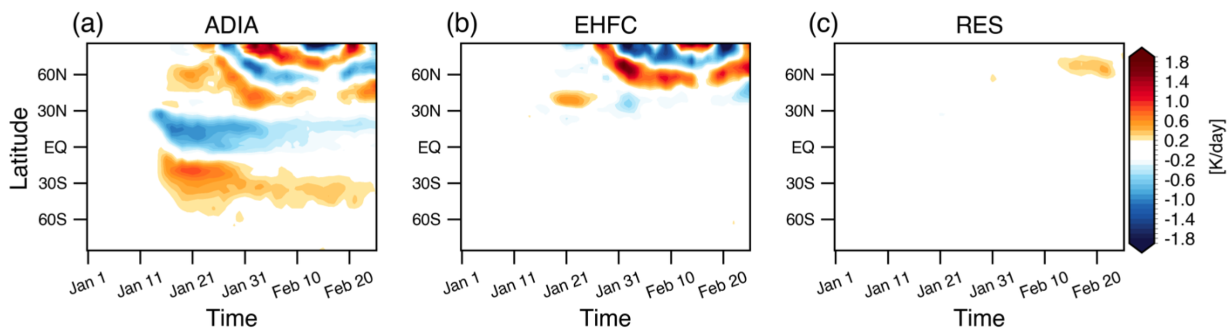

Figure S1. As in Fig. 2, but for the (a) adiabatic process by vertical motion (ADIA), (b) meridional eddy heat flux convergence (EHFC), and (c) the residual term (RES).

Figure 2 summarizes the evolution of the temperature tendency following the soot injection. The net temperature tendency (Fig. 2a) is well captured by the sum of the diagnosed radiative and dynamical terms (Fig. 2b), indicating that the heat-budget decomposition provides a physically consistent explanation of the temperature response. The atmosphere warms rapidly over the tropics within a few days of the injection (January 12-15), and a secondary warming signal emerges in the extratropics roughly two weeks later.

Figs. 2c and 2d show the separate contributions of radiative and dynamical processes to the temperature tendency. Fig. S1 provides a detailed breakdown of the individual contributions from adiabatic process (ADIA), meridional eddy heat-flux convergence (EHFC), and the residual terms (RES) to the dynamical tendency. The radiative and dynamical contributions exhibit distinct spatial structures (Figs. 2c-2d). Radiative heating produces strong tropical warming, consistent with shortwave absorption by black-carbon aerosols, but this radiative signal remains confined largely within ±30° latitude. In contrast, the dynamical tendency exhibits cooling over the tropics - associated with enhanced ascent and adiabatic cooling (Fig. S1a) - and warming over the midlatitudes (Fig. 2d). The dynamical warming over the mid-to-high latitudes arises from both vertical motion (ADIA) and meridional heat transport by atmospheric eddies (EHFC), as shown in Fig. S1.

Taken together, the results indicate that aerosol perturbations influence the temperature field through two pathways: (1) direct radiative heating in the tropics and (2) dynamical heat redistribution that transports warm anomalies poleward. The latter dominates the extratropical response and is therefore central to understanding how the soot injection alters the meridional temperature structure.

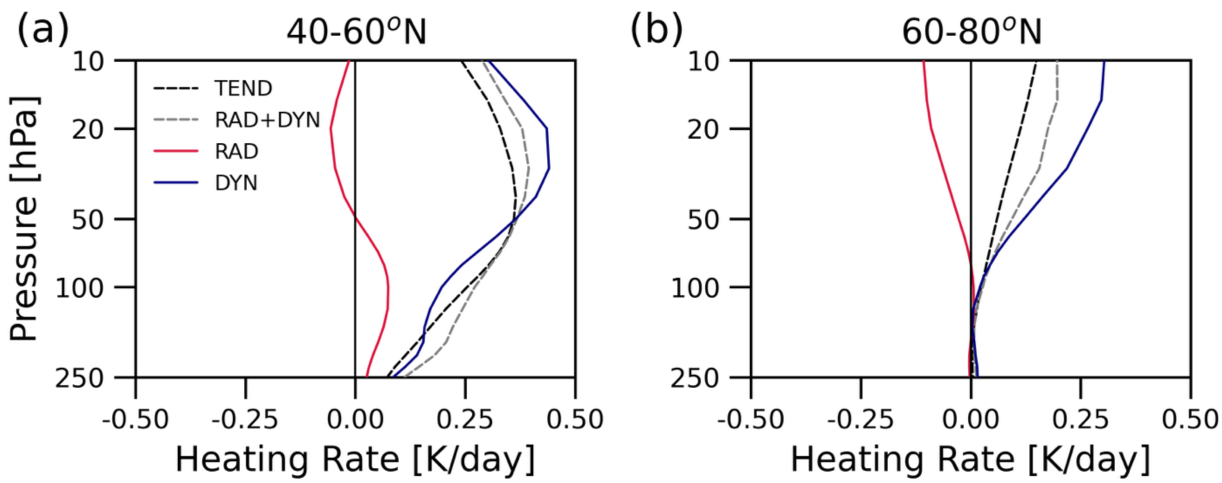

Figure 3. Vertical profiles of temperature-tendency averaged over (a) 40-60°N and (b) 60-80°N. The net temperature tendency (TEND) is shown in black dashed, the sum of radiative and dynamical tendencies (RAD+DYN) in gray dashed, radiative heating (RAD) in red, and dynamical heating (DYN) in blue line.

3.3. Mechanisms for Stratospheric Polar Vortex Response

Figure 3 summarizes the vertical structure of the temperature tendencies over the NH mid- and high latitudes. Again, the close agreement between the net temperature tendency and the sum of the radiative and dynamical terms (black and gray dashed lines) indicates that the heat-budget analysis accurately captures the processes driving the temperature response.

Both latitude bands show warming, but with a pronounced meridional contrast. The midlatitudes (40–60°N; Fig. 3a) warm more strongly than the high latitudes (60–80°N; Fig. 3b), implying an increase in the meridional temperature gradient. Through thermal-wind balance, this enhanced temperature gradient is consistent with the strengthening of the polar jet noted in Fig. 1b. The warming at both latitude ranges is dominated by dynamical processes (blue lines), in agreement with the time-evolving dynamical heating patterns shown in Fig. 2. These results underscore that large-scale circulation anomalies - not direct radiative heating - govern the extratropical temperature structure and play the key role in the early strengthening of the polar vortex.

To further diagnose the circulation response, we examine the zonal-mean momentum budget as follows (Eq. 2; Holton, 2004; Dima et al., 2005; White et al., 2024):

$$\frac{\partial \bar{U}}{\partial t} \cong \bar{v}\left(f - \frac{1}{a\cos\phi}\frac{\partial(\bar{u}\cos\phi)}{\partial\phi}\right) - \frac{1}{a\cos^2\phi}\frac{\partial\left(\cos\phi\left(\overline{u'v'}\right)\right)}{\partial\phi} - \left(\bar{u}\frac{\partial\bar{\omega}}{\partial p} + \frac{\partial\left(\overline{u'\omega'}\right)}{\partial p} - \bar{F}_r\right) \ldots (2)$$

COR EMFC URES

The wind tendency can be written as the sum of three terms, the Coriolis acceleration (COR), the eddy momentum flux convergence (EMFC), and the and the residual term (URES), which includes vertical advection, vertical eddy momentum flux convergence, and friction (F_r).

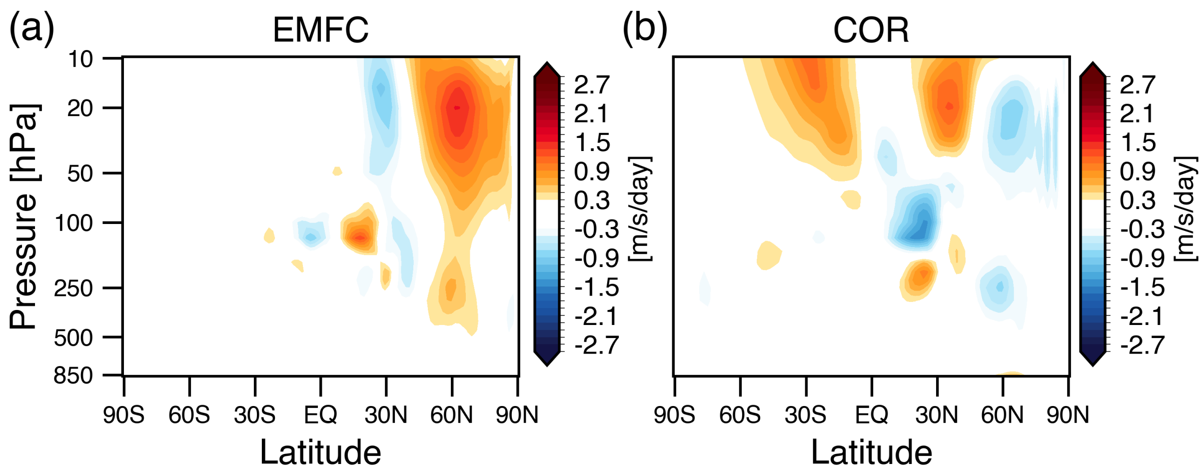

Figure 4. The acceleration of the zonal-mean zonal flow (m s^{-1} day^{-1}) associated with the (a) eddy momentum-flux convergence (EMFC) and (b) Coriolis torque (COR).

Figure 4 demonstrates the key components of the zonal-mean momentum budget that drive the anomalous zonal wind responses. The eddy momentum-flux convergence produces strong westerly accelerations throughout the stratosphere across ~40-90°N (Fig. 4a), indicating that eddy forcing is the primary driver of the anomalous zonal-wind response. The spatial structure of the EMFC anomalies aligns with the regions of strengthened westerlies in Fig. 1b, consistent with enhanced wave-mean flow interactions contributing to the intensification of the polar vortex.

The Coriolis torque contributes more modestly to the anomalies over the NH mid-to-high latitudes, indicating a slight equatorward shift of the zonal-wind anomalies. The influence of the Coriolis torque is more pronounced over the SH subtropics and midlatitudes, where the jet intensifies but the EMFC anomalies are weak (Fig. 4b). Overall, the results in Fig. 4 reveal the dynamical pathway for the polar-jet acceleration, highlighting the key role of eddy momentum forcing.

4. Conclusions

This study uses a chemistry–climate model to examine the transient wintertime circulation response to soot injected into the tropical stratosphere during a regional-scale nuclear conflict. Previous studies of stratospheric aerosol injection scenario showed that the aerosol-induced stratospheric heating anomalies are linked to strengthening of the winter polar vortex through three broad pathways:

(1) **Direct radiative mechanism:** Aerosol-induced tropical warming enhances the meridional temperature gradient and strengthens the jet through thermal-wind balance (Graf et al., 1993; Kodera, 1994; Robock & Mao, 1995; Coupe & Robock, 2021).

(2) **Indirect dynamical mechanism:** The radiative temperature anomalies are often confined to the subtropics, which primarily strengthens the subtropical jet. The enhanced subtropical jet deflects planetary-wave propagation equatorward, reduces poleward wave fluxes, and indirectly intensifies the polar vortex (Toohey et al., 2014; Bittner et al., 2016; Dalla Santa et al., 2019).

(3) **Indirect radiative mechanism:** Aerosol scattering cools the surface and weakens the tropospheric meridional temperature gradient and baroclinicity, reducing upward wave flux and further contributing to polar-jet acceleration (Graf et al., 1992; Stenchikov et al., 2002; Dalla Santa et al., 2019).

Here, we quantify the stratospheric heat and momentum budgets to assess the transient thermal and dynamical responses of the circulation to the aerosol perturbations during the month following the injection. The heat budget reveals that tropical warming is driven by radiative heating, whereas extratropical warming arises primarily from dynamical processes that cool the tropics and transport heat poleward (Fig. 2). These extratropical warm anomalies driven by dynamical processes enhance the meridional temperature gradient over the polar-jet region (Fig. 3). The momentum budget (Fig. 4) further shows that the strengthening of the polar vortex is driven primarily by eddy momentum-flux convergence.

Our results provide a new perspective, a **direct dynamical mechanism** – for how stratospheric aerosol perturbations influence atmospheric circulation in remote regions. The transient dynamical response to the aerosol perturbation can play a key role in strengthening the winter polar jet, through the redistribution of heat and the transport of momentum.

Acknowledgments

S. S and S. Y. are supported by a grant from the Future of Life Institute. The CESM project is supported primarily by the U.S. National Science Foundation. The authors acknowledge the Climate Simulation Laboratory at NCAR's Computational and Information Systems Laboratory (CISL; sponsored by NSF and other agencies) and the MIT's Massachusetts Green High Performance Computing Center (supported by the Center for Sustainability Science and Strategy) for providing computing and storage resources. Open Access funding enabled and organized by MIT Hybrid 2025.

A conflict of interest disclosure statement

All authors declare that they have no conflicts of interest.

Open Research

The data used in the generation of the figures of this paper are available in Yook (2025). WACCM4 is an open-source community model, which was developed with support primarily from the National Science Foundation, see Marsh et al. (2013).

References

Alh